

# ROAST: Rollout-based On-distribution Activation Steering Technique

Xuanbo Su<sup>1</sup> Hao Luo<sup>1</sup> Yingfang Zhang<sup>2</sup> Lijun Zhang<sup>1</sup>

<sup>1</sup>Bairong Inc., Beijing, China

<sup>2</sup>School of Mathematics, Harbin Institute of Technology, Harbin, China

Correspondence: [lijun.zhang@brgroup.com](mailto:lijun.zhang@brgroup.com)

## Abstract

Activation steering provides parameter-efficient control over large language models (LLMs) at inference time, but many methods rely on off-distribution supervision and discrete masking, leading to brittle interventions. We propose **ROAST** (Rollout-based On-distribution Activation Steering Technique), which estimates steering directions from the model’s own on-distribution rollouts via **ROC** and avoids hard sparsification via **Continuous Soft Scaling (CSS)** and **Grouped Mean Normalization**. Our empirical analysis reveals that while activation magnitude correlates moderately with directional consistency, the variance in magnitude is significant and often disproportionate to semantic quality. This suggests that high-magnitude activations risk dominating the global steering direction if not properly normalized. To address this, ROAST employs grouped normalization to balance contributions across samples, ensuring a more robust estimation of the consensus steering direction. Across models (0.6B to 32B), ROAST consistently improves performance on diverse tasks (e.g., +9.7% on GSM8K for Qwen3-0.6B and +12.1% on TruthfulQA for GLM4-32B), and analyses show that CSS better preserves activation energy.

## 1 Introduction

Large Language Models (LLMs) achieve strong performance across tasks, yet controlling their behavior remains difficult. Dominant alignment pipelines—instruction tuning (e.g., FLAN (Wei et al., 2022)) and preference-based fine-tuning (e.g., RLHF (Bai et al., 2022))—are expensive and provide limited, post-hoc control at inference time. Activation steering (Turner et al., 2024; Rimsky et al., 2024; Zou et al., 2025; Stolfo et al., 2025) offers a lightweight alternative by intervening directly on internal representations during decoding. However, existing steering methods are brittle: they suffer

from extraction-deployment distribution shift and discard information via discrete sparsification (e.g., Top- $k$  masking) (Rimsky et al., 2024; Wang et al., 2025; Li et al., 2024).

We propose **ROAST** (Rollout-based On-distribution Activation Steering Technique), which addresses these challenges by grounding steering vector extraction in statistical moment estimation under the model’s autoregressive distribution. Key contributions include:

- **ROC:** Samples rollouts to reduce distribution-induced bias and obtain a more reliable estimate of the steering direction under the model’s natural distribution.
- **CSS:** Replaces discrete masking with continuous normalization, serving as a variance-constrained estimator that preserves signal energy.

ROAST consistently outperforms prior steering baselines across multiple benchmark tasks and model sizes, particularly on reasoning tasks, and often matches or exceeds few-shot performance.

## 2 Related Work

Activation steering modifies model behavior by intervening on internal representations at inference time (Turner et al., 2024; Rimsky et al., 2024; Zou et al., 2025; Stolfo et al., 2025). This line of work is motivated by the observation that many semantic and behavioral attributes are approximately linear in activation space, making simple geometric operations effective for probing and steering (Park et al., 2024). A common approach is to extract a *contrastive direction* from paired executions, e.g., by contrasting prompts (Turner et al., 2024; Zou et al., 2025; Liu et al., 2024; Subramani et al., 2022) or contrasting answers (CAA) (Rimsky et al., 2024); related instruction-following work similarly uses difference vectors between instruction-present and

instruction-absent runs (Stolfo et al., 2025). Another line uses probes to localize causal components (e.g., attention heads) and then intervenes on those components directly (Li et al., 2024; Chen et al., 2024). Interventions are typically applied either as vector addition in the residual stream (Rimsky et al., 2024) or as component-wise edits such as head-level intervention (Li et al., 2024) or element-wise scaling with discrete masks (SADI) (Wang et al., 2025).

ROAST is closest to contrastive direction methods (e.g., CAA (Rimsky et al., 2024)), but differs in two robustness-oriented aspects. First, instead of extracting directions from teacher-forced trajectories and applying them to free-running generation, ROAST estimates directions from on-distribution rollouts (ROC) to better match the inference-time activation distribution. Second, rather than relying on discrete sparsification such as Top-K masking in SADI (Wang et al., 2025), ROAST uses continuous soft scaling (CSS) to preserve full-dimensional activation energy while controlling intervention magnitude.

### 3 Observations and Motivation

Before presenting our framework, we investigate the fundamental limitations of existing steering methods through three key empirical observations. These observations directly motivate the design of ROAST.

#### 3.1 Distributional Shift in Teacher-Forcing

Existing methods typically extract steering vectors from teacher-forced activations ( $p_{tf}$ ) but apply them during free-running generation ( $p_{ar}$ ). However, as illustrated in Figure 1, these two regimes exhibit a significant distributional shift. By analyzing MLP activations at the sequence boundary across 64 samples from GSM8K (Cobbe et al., 2021), we observe that mean activations conditioned on teacher-forced versus autoregressive prefixes are poorly aligned. Specifically, the cosine similarity significantly deviates from unity in early and middle layers, while the relative  $L_2$  distance remains non-negligible throughout the network. These results suggest that teacher-forced vectors may reside on a latent manifold that is misaligned with the model’s actual inference-time distribution, motivating the on-distribution estimation approach advocated in recent work (Rimsky et al., 2024; Li et al., 2024).

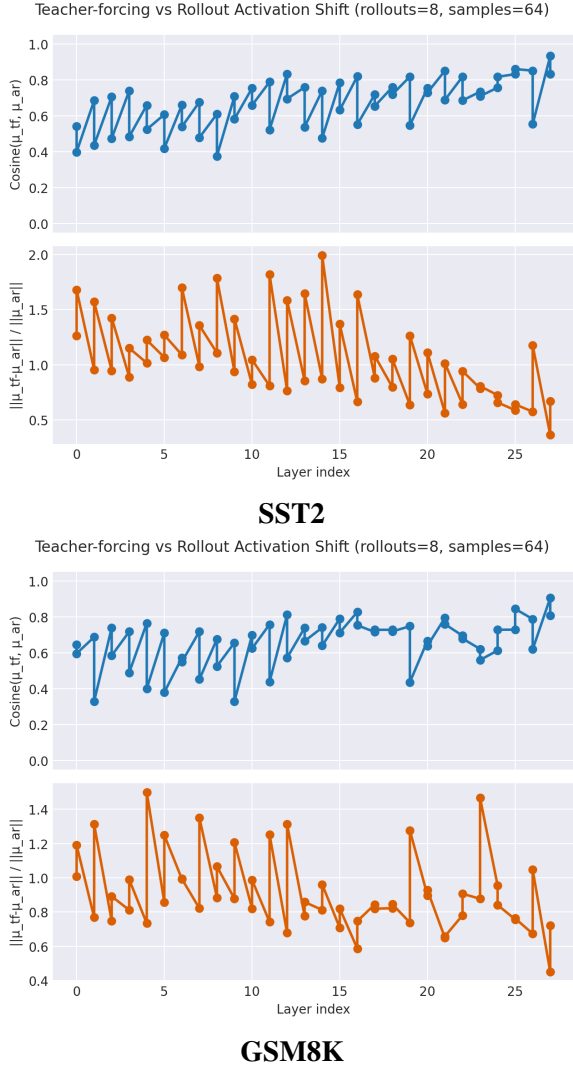


Figure 1: Quantifying activation distribution shift between teacher-forcing and rollouts (Qwen3-0.6B) in MLP activation. Cosine similarity  $\cos(\mu_{tf}, \mu_{ar})$  and relative  $L_2$  difference are calculated between the mean activation vectors  $\mu_{tf}$  and  $\mu_{ar}$ , respectively.

#### 3.2 Information Loss in Sparse Masking

Methods employing discrete Top-K masking to enforce sparsity often discard significant signal energy. As quantified in Figure 2, the top 10% of dimensions capture only about half of the total  $L_2$  energy. By zeroing out the remaining 90% of dimensions, these methods lose substantial representational signal, which motivates our Continuous Soft Scaling (CSS) approach to preserve full-dimensional energy. This observation is consistent with prior work highlighting the presence of extremely large activation outliers (“massive activations”) in LLMs, which can dominate naive aggregation and motivate magnitude-aware normalization (Sun et al., 2024).

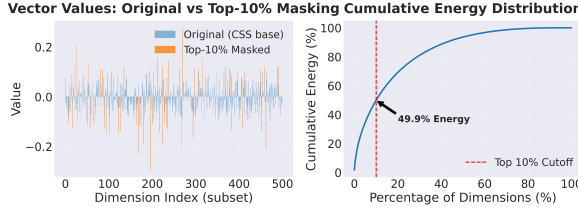


Figure 2: Sparse masking versus CSS (Qwen3-8B on SST2). **Left:** Top-10% masking zeros out 90% of dimensions. **Right:** Cumulative energy distribution shows the top 10% of dimensions capture only  $\sim 50\%$  of the total energy, leading to massive information loss in discrete masking.

### 3.3 Magnitude and Quantity Imbalance

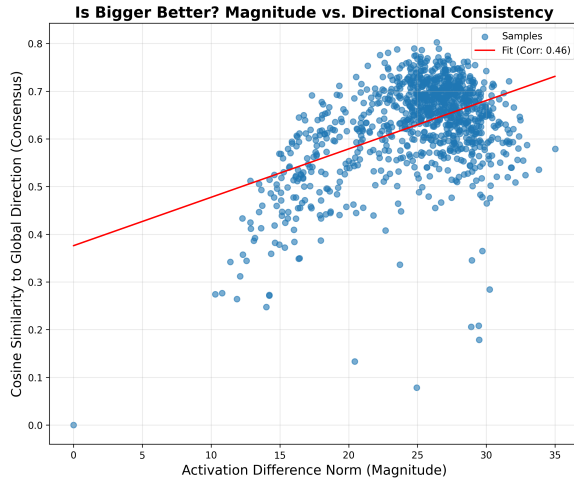


Figure 3: Relationship between activation magnitude and directional consistency (Qwen3-8B on GSM8k with layer 16). Magnitudes correlate moderately with consistency ( $\rho \approx 0.46$ ) but exhibit extreme variance, consistent with outlier feature observations. Unnormalized aggregation risks domination by high-magnitude samples regardless of semantic quality.

We identify two critical sources of bias that render naive aggregation suboptimal:

**Magnitude Imbalance:** Magnitudes correlate moderately with directional consistency ( $\rho \approx 0.46$ , Figure 3) but exhibit extreme variance compared to bounded consistency scores. This heavy-tailed distribution (consistent with outlier features (Sun et al., 2024)) risks allowing high-magnitude samples to dominate the steering direction regardless of quality. Grouped normalization mitigates this by balancing contributions.

**Quantity Imbalance:** The number of valid contrastive pairs varies per question depending on the model’s performance (e.g., harder questions yield

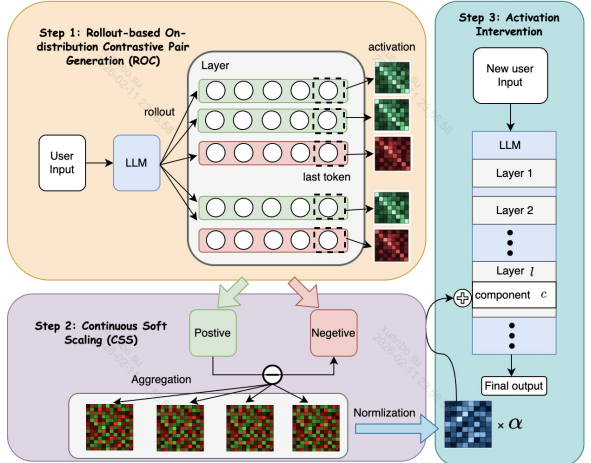


Figure 4: Overview of ROAST. **Step 1 (ROC):** Sample on-distribution rollouts, extract activations at the last token, and form contrastive positive/negative pairs. **Step 2 (CSS):** Aggregate contrastive activation differences and apply continuous soft scaling via normalization to obtain a steering direction. **Step 3:** During inference, add the resulting steering vector (scaled by strength  $\alpha$ ) to a chosen layer  $l$  and component  $c$  (e.g., MLP or Attention) to steer model outputs.

fewer correct responses). A naive average over all pairs assigns more weight to questions that are easier to contrast (generating more pairs), introducing a sampling bias.

These observations directly motivate our **Continuous Soft Scaling (CSS)** to handle magnitude variance and **Grouped Mean Normalization** ("One Question, One Vote") to mitigate sampling bias.

## 4 The ROAST Framework

Motivated by these observations, we propose ROAST (Figure 4), a three-stage framework comprising: (1) **Rollout-based On-distribution Contrastive Pair Generation (ROC)**, (2) **Continuous Steering Vector Estimation** via CSS, and (3) **Activation Intervention** during inference.

### 4.1 Rollout-based On-distribution Contrastive Pair Generation (ROC)

To address the distributional shift observed in Section 3.1, ROAST utilizes model-generated rollouts to construct contrastive pairs, drawing samples directly from  $p_{\text{par}}$ .

We first obtain on-distribution contrastive rollouts and extract the last-token activations; we then aggregate and normalize their differences to estimate a stable steering direction; finally, we inject the scaled vector into the residual stream at a se-

lected layer and component during generation.

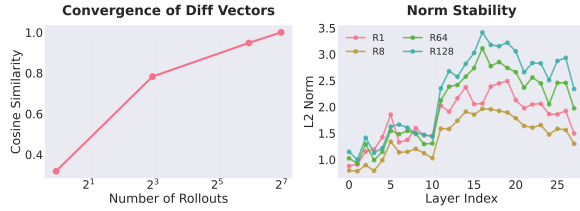


Figure 5: Rollout stability analysis on Qwen3-0.6B. **Left:** Steering vectors converge as rollout count increases. **Right:** Layer-wise  $L_2$  norms remain stable across different rollout counts.

As shown in Figure 5, the extracted steering vectors converge quickly as the number of rollouts increases, achieving high cosine similarity with the 128-rollout reference even at  $n = 64$ . For a given training query  $q$ , the ROC process proceeds as follows (see Algorithm 1 and Appendix A.1 for implementation details):

- 1. Generative Rollout:** We sample  $n$  diverse responses  $\mathcal{R} = \{r_1, \dots, r_n\}$  from  $p_{\text{par}}(\cdot | q)$ .
- 2. Outcome-based Partitioning:** Responses are categorized as correct ( $r^+$ ) or incorrect ( $r^-$ ) via a verifier  $\mathcal{V}(r, a^*)$ .
- 3. Contrastive Pair Formation:** We construct the set  $\mathcal{P} = \{(r^+, r^-) : r^+ \in \mathcal{R}^+, r^- \in \mathcal{R}^-\}$ .

The raw steering direction  $\Delta h$  is estimated as:

$$\Delta h = \frac{1}{|\mathcal{R}^+|} \sum_{r^+ \in \mathcal{R}^+} h(q, r^+) - \frac{1}{|\mathcal{R}^-|} \sum_{r^- \in \mathcal{R}^-} h(q, r^-) \quad (1)$$

where  $h(q, r)$  is the activation at the final token position.

## 4.2 Continuous Soft Scaling (CSS)

To mitigate the information loss described in Section 3.2, ROAST replaces discrete masking with **Continuous Soft Scaling (CSS)**. Instead of truncating dimensions, we normalize the difference vector:

$$v_{\text{CSS}} = \text{Norm}(\Delta h) \quad (2)$$

We experiment with both  $L_2$  normalization and max-norm (i.e.,  $L_\infty$ ) normalization; unless otherwise specified, we use  $L_2$  normalization, which preserves directional information while ensuring numerical stability (see Appendix E for additional methodological details). From a robust estimation perspective, normalization can also be viewed

as mitigating the influence of activation outliers, aligning with classical treatments of robust statistics (Huber and Ronchetti, 2009).

## 4.3 Grouped Mean Normalization

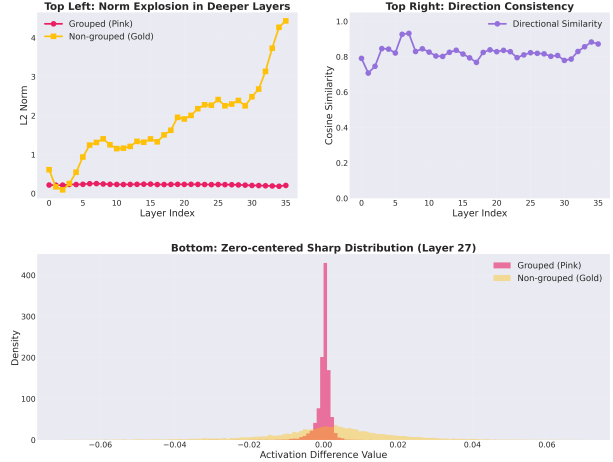


Figure 6: Impact of Grouped Mean Normalization (Qwen3-8B on MMLU with MLP activation). **Top Left:** Without grouping (gold), difference vector norms explode in deeper layers, whereas grouped normalization (pink) maintains stable magnitudes. **Top Right:** The direction remains relatively consistent ( $\cos \approx 0.8$ ), indicating that grouping primarily stabilizes scale. **Bottom:** Grouping produces a sharper, zero-centered distribution of difference values, effectively mitigating outlier dominance.

To address the sampling bias and numerical instability observed in rollout aggregation, we introduce a "One Question One Vote" strategy. As illustrated in Figure 6, simply averaging all rollout pairs (Non-grouped) leads to a drastic explosion in vector norms in deeper layers, particularly for attention outputs where norms can exceed  $10 \times$  the stable range.

We first compute normalized mean vectors for each question, where  $Q$  denotes the set of questions in the steering dataset:

$$\bar{v}_q = \text{Norm} \left( \frac{1}{|\mathcal{P}_q|} \sum_{(r^+, r^-) \in \mathcal{P}_q} (h(r^+) - h(r^-)) \right)$$

We then average across questions and apply a final normalization:  $v_{\text{final}} = \text{Norm} \left( \frac{1}{|Q|} \sum_{q \in Q} \bar{v}_q \right)$ . This ensures that questions with many valid rollout pairs do not dominate the global steering direction and prevents the norm explosion driven by high-variance outliers. We provide additional intuition for this two-stage normalization in Appendix B,

along with ablation studies in Table 10. Viewed through the lens of our introduction’s statistical moment estimation framing, this procedure can be interpreted as an empirical first-moment (mean) estimator under the model’s rollout distribution, where the per-question normalization serves as a robustness mechanism.

#### 4.4 Activation Intervention

During inference, we apply the steering vector to the original activation  $h^{(l,c)}$  with strength  $\alpha$ :

$$h'^{(l,c)} = h^{(l,c)} + \alpha \cdot v_{\text{final}}^{(l,c)} \quad (3)$$

Our ablations confirm that intervening on MLP activations across all layers yields the most robust performance.

### 5 Experiments

#### 5.1 Experimental Setup

**Models:** We evaluate on Qwen3 series (0.6B, 8B, 14B, 32B parameters) (Yang et al., 2025) and GLM4 series (9B, 32B parameters) (GLM et al., 2024), as well as Gemma3-1B (Team et al., 2025). This selection covers a wide range of model scales and diverse architectures, demonstrating the generalizability of ROAST across different foundation models.

**Datasets and Metrics:** We test on 9 datasets spanning Truthfulness (TruthfulQA; Lin et al., 2022), Instruction Following (IFEval; Zhou et al., 2023), Sentiment Analysis (SST2, SST5; Socher et al., 2013), Reasoning (MMLU, Hendrycks et al., 2021a; GSM8K, Cobbe et al., 2021; MATH500, Hendrycks et al., 2021b), and Commonsense (Winogrande, Sakaguchi et al., 2021; XNLI, Conneau et al., 2018). We report accuracy or task-specific metrics; full experimental settings, evaluation procedure, and implementation details are provided in Appendix A.

**Baselines:** We compare against:

- **Baseline:** No intervention (base model performance)
- **Few-shot:** Using training examples as in-context demonstrations (100 examples when applicable)
- **CAA:** Contrastive Activation Addition (Rimsky et al., 2024)
- **SADI:** Semantics-Adaptive Activation Intervention (Wang et al., 2025)

**Hyperparameters:** We use task-specific rollout counts (64 for base-mode, 8 for chat-mode) and tune the intervention strength  $\alpha$  via grid search. Unless otherwise stated, we extract the steering vector from the final token position and apply it during decoding by adding it to the MLP activations for the first generated token, across all layers. Baselines are tuned following their original paper recommendations to ensure fair comparison. Detailed hyperparameter configurations, including rollout settings, grid search ranges, and baseline tuning parameters, are provided in Appendix A. Unless otherwise specified, results are reported as the mean and standard deviation across 2 random seeds (42, 52); for selected ablations we additionally report statistics over 3 seeds (42, 22, 52). All evaluations use greedy decoding to ensure reproducibility.

#### 5.2 Main Results

Table 1 presents a comprehensive comparison of ROAST against baseline and existing intervention methods across diverse model architectures and datasets. Our results demonstrate that ROAST consistently achieves superior performance, often matching or exceeding few-shot learning without requiring in-context demonstrations at inference time.

**Performance across Scales:** ROAST yields consistent improvements across model sizes. On Qwen3-0.6B, ROAST improves the average score by +4.02% over the baseline and by +5.76% over CAA, while SADI underperforms the baseline (40.54–44.49 vs. 46.01). Gains are especially pronounced on SST2 (+6.44%) and MMLU (+5.24%). On Qwen3-8B, ROAST remains effective, achieving 70.22% average accuracy and slightly outperforming 100-shot ICL (70.06%), whereas SADI remains below the baseline (65.90–66.12 vs. 67.35). Across seeds, ROAST also exhibits lower variance than few-shot and prior steering baselines, indicating more stable steering directions.

**On-Distribution Advantage:** A key finding is the significant performance gap between ROAST and CAA. Across all tested models, CAA often exhibits performance degradation (e.g., -13.59% on TruthfulQA for Qwen3-0.6B), consistent with the hypothesis that the distribution shift between teacher-forced training pairs and the model’s natural generation distribution impairs steering. By utilizing on-distribution rollouts (ROC), ROAST effectively mitigates this shift, resulting in stable

Model	Method	SST2	SST5	MMLU	TruthfulQA	Winogrande	XNLI	Avg
Qwen3-0.6B	Baseline	78.80 $\pm$ 0.29	25.65 $\pm$ 0.30	35.49 $\pm$ 0.01	48.78 $\pm$ 0.52	49.80 $\pm$ 0.59	37.54 $\pm$ 0.12	46.01
	Few-shot-100	84.03 $\pm$ 0.38	<b>30.07</b> $\pm$ <b>1.63</b>	<u>40.20</u> $\pm$ <u>0.05</u>	48.21 $\pm$ 0.11	49.49 $\pm$ 0.08	44.15 $\pm$ 0.02	49.36
	CAA-100	79.08 $\pm$ 1.10	28.76 $\pm$ 0.00	35.55 $\pm$ 0.01	35.19 $\pm$ 0.00	49.80 $\pm$ 0.00	37.22 $\pm$ 0.01	44.27
	CAA-1000	78.55 $\pm$ 0.25	28.73 $\pm$ 0.02	35.81 $\pm$ 0.01	35.19 $\pm$ 0.00	49.80 $\pm$ 0.00	37.13 $\pm$ 0.01	44.20
	SADI-100	80.52 $\pm$ 0.11	25.90 $\pm$ 0.39	37.71 $\pm$ 0.05	33.19 $\pm$ 0.12	<u>50.49</u> $\pm$ <u>0.02</u>	15.46 $\pm$ 0.06	40.54
	SADI-1000	82.81 $\pm$ 0.03	28.08 $\pm$ 0.03	<u>38.16</u> $\pm$ <u>0.04</u>	24.13 $\pm$ 0.08	<u>49.85</u> $\pm$ <u>0.06</u>	43.92 $\pm$ 0.02	44.49
	ROAST-100 (group)	<b>85.24</b> $\pm$ <b>0.13</b>	<u>29.89</u> $\pm$ <u>0.58</u>	<b>40.73</b> $\pm$ <b>0.02</b>	49.22 $\pm$ 0.16	49.65 $\pm$ 0.08	45.47 $\pm$ 0.01	<b>50.03</b>
	ROAST-100 (no-group)	85.03 $\pm$ 0.32	<u>29.27</u> $\pm$ <u>0.40</u>	37.32 $\pm$ 0.10	47.47 $\pm$ 0.42	49.95 $\pm$ 0.03	<u>46.26</u> $\pm$ <u>0.02</u>	49.22
	ROAST-1000 (group)	84.60 $\pm$ 0.38	27.91 $\pm$ 0.14	38.15 $\pm$ 0.01	<b>49.91</b> $\pm$ <b>0.23</b>	<b>52.36</b> $\pm$ <b>0.00</b>	41.72 $\pm$ 0.01	49.11
	ROAST-1000 (no-group)	84.81 $\pm$ 0.21	27.23 $\pm$ 0.20	37.32 $\pm$ 0.01	<u>49.39</u> $\pm$ <u>0.12</u>	49.75 $\pm$ 0.03	42.59 $\pm$ 0.12	48.52
Qwen3-8B	Baseline	86.68 $\pm$ 0.21	38.12 $\pm$ 0.58	66.99 $\pm$ 0.01	78.66 $\pm$ 0.16	64.29 $\pm$ 0.03	69.37 $\pm$ 0.01	67.35
	Few-shot-100	86.81 $\pm$ 0.11	<b>50.42</b> $\pm$ <b>0.31</b>	<b>71.82</b> $\pm$ <b>0.03</b>	72.66 $\pm$ 0.18	<b>67.84</b> $\pm$ <b>0.13</b>	<b>70.84</b> $\pm$ <b>0.03</b>	<u>70.06</u>
	CAA-100	86.52 $\pm$ 0.13	24.82 $\pm$ 0.02	67.08 $\pm$ 0.01	74.11 $\pm$ 0.00	64.30 $\pm$ 0.01	53.02 $\pm$ 0.00	61.64
	CAA-1000	86.75 $\pm$ 0.01	34.82 $\pm$ 0.01	67.13 $\pm$ 0.01	74.72 $\pm$ 0.00	64.30 $\pm$ 0.01	53.02 $\pm$ 0.00	63.46
	SADI-100	87.25 $\pm$ 0.01	39.39 $\pm$ 0.01	66.93 $\pm$ 0.02	72.28 $\pm$ 0.15	61.34 $\pm$ 0.01	69.56 $\pm$ 0.01	66.12
	SADI-1000	86.32 $\pm$ 0.01	38.40 $\pm$ 0.01	66.56 $\pm$ 0.02	73.24 $\pm$ 0.03	61.09 $\pm$ 0.00	69.80 $\pm$ 0.00	65.90
	ROAST-100 (group)	<b>89.90</b> $\pm$ <b>0.00</b>	39.11 $\pm$ 0.13	67.71 $\pm$ 0.02	<u>81.18</u> $\pm$ <u>0.04</u>	<u>65.43</u> $\pm$ <u>0.01</u>	69.34 $\pm$ 0.00	68.78
	ROAST-100 (no-group)	89.11 $\pm$ 0.00	43.83 $\pm$ 0.01	69.06 $\pm$ 0.00	80.14 $\pm$ 0.00	65.24 $\pm$ 0.07	69.50 $\pm$ 0.01	69.48
	ROAST-1000 (group)	88.47 $\pm$ 0.01	<u>48.17</u> $\pm$ <u>0.15</u>	69.11 $\pm$ 0.02	<b>81.62</b> $\pm$ <b>0.03</b>	64.64 $\pm$ 0.01	69.29 $\pm$ 0.00	<b>70.22</b>
	ROAST-1000 (no-group)	89.11 $\pm$ 0.01	43.47 $\pm$ 0.02	<u>69.31</u> $\pm$ <u>0.01</u>	79.70 $\pm$ 0.02	65.13 $\pm$ 0.01	69.26 $\pm$ 0.01	69.33
Gemma3-1B	Baseline	81.08 $\pm$ 0.11	40.02 $\pm$ 0.28	39.09 $\pm$ 0.01	19.25 $\pm$ 0.04	50.59 $\pm$ 0.08	41.80 $\pm$ 0.01	45.30
	Few-shot-100	84.05 $\pm$ 0.00	<u>43.36</u> $\pm$ <u>0.01</u>	37.58 $\pm$ 0.01	<u>22.32</u> $\pm$ <u>0.00</u>	47.71 $\pm$ 0.00	48.66 $\pm$ 0.00	47.28
	CAA-100	82.69 $\pm$ 0.10	<u>40.15</u> $\pm$ <u>2.26</u>	39.51 $\pm$ 1.34	21.33 $\pm$ 0.45	50.27 $\pm$ 1.34	<u>47.54</u> $\pm$ <u>3.18</u>	46.91
	CAA-1000	82.09 $\pm$ 2.15	42.31 $\pm$ 0.45	39.15 $\pm$ 0.38	18.82 $\pm$ 0.87	50.79 $\pm$ 1.08	43.10 $\pm$ 0.56	46.04
	SADI-100	84.96 $\pm$ 1.86	21.75 $\pm$ 0.14	<b>40.38</b> $\pm$ <b>0.41</b>	19.25 $\pm$ 0.44	48.32 $\pm$ 0.39	42.20 $\pm$ 3.62	42.81
	SADI-1000	<b>85.10</b> $\pm$ <b>1.86</b>	20.48 $\pm$ 0.28	38.42 $\pm$ 0.60	19.77 $\pm$ 1.31	47.39 $\pm$ 1.53	42.10 $\pm$ 0.04	42.21
	ROAST-100 (group)	81.95 $\pm$ 2.29	<b>43.50</b> $\pm$ <b>0.06</b>	39.87 $\pm$ 0.44	19.43 $\pm$ 2.53	<u>51.13</u> $\pm$ <u>0.94</u>	47.68 $\pm$ 3.84	47.26
	ROAST-100 (no-group)	81.23 $\pm$ 1.58	<b>43.50</b> $\pm$ <b>0.34</b>	39.68 $\pm$ 0.01	19.86 $\pm$ 0.35	<u>51.28</u> $\pm$ <u>0.20</u>	45.63 $\pm$ 0.73	46.86
	ROAST-1000 (group)	84.31 $\pm$ 5.58	42.65 $\pm$ 0.39	40.20 $\pm$ 0.37	<b>23.47</b> $\pm$ <b>3.57</b>	<u>52.02</u> $\pm$ <u>1.67</u>	44.29 $\pm$ 0.11	<b>47.82</b>
	ROAST-1000 (no-group)	83.10 $\pm$ 0.01	41.35 $\pm$ 0.01	<u>39.91</u> $\pm$ <u>0.07</u>	22.77 $\pm$ 0.01	<b>52.56</b> $\pm$ <b>0.01</b>	<b>48.84</b> $\pm$ <b>0.01</b>	<b>48.09</b>

Table 1: Main results across multiple models and benchmarks. Values denote accuracy (%)  $\pm$  standard deviation across 2 random seeds. **Bold**, underlined, and *italic* indicate the best, second-best, and third-best results, respectively. We compare ROAST against few-shot prompting and prior activation steering baselines (CAA and SADI), and report grouped versus non-grouped aggregation and 100/1000 training sizes for ROAST.

and positive steering across most benchmarks.

**Complex Reasoning and Instruction Following:** Table 2 evaluates performance on multi-step reasoning (GSM8K, MATH500) and instruction following (IFEval). ROAST demonstrates remarkable gains on GSM8K for Qwen3-0.6B (+9.66% absolute improvement), where reasoning paths are often fragile and highly sensitive to distributional shifts. For stronger models like Qwen3-8B, ROAST enhances IFEval performance by 3.15%, indicating its ability to refine instruction-following capabilities even in highly capable foundation models. It is important to note that for these chat-mode evaluations, the few-shot baseline is restricted to 20 examples to stay within the model’s context length limits, whereas ROAST provides a more scalable and effective alternative that does not consume the context window. Furthermore, the low variance in ROAST’s performance across different rollout sets underscores its advantage in identifying robust, task-specific steering directions that are less susceptible to the choice of training samples.

### 5.3 Ablation Studies

We present ablations to isolate the contributions of ROAST’s core components and design choices.

By comparing the teacher-forced baseline (Table 4) with ROC variants (Table 7), we can decouple the gains from ROC and CSS. On SST2, ROC alone (without normalization) improves over teacher-forcing by 4.15% (78.51%  $\rightarrow$  82.66%), while adding CSS contributes a further 2.58% (82.66%  $\rightarrow$  85.24%). Their combination yields a total gain of 6.73%, confirming the importance of both on-distribution extraction and effective normalization. We ablate the intervention component (Table 3) and scaling/normalization variants (Table 7, including removing normalization). Performance is relatively insensitive to the rollout count once it is moderately large (Table 4), and steering is most effective when applied to all layers (Table 6). We summarize key findings on component selection, rollout count, anchor position (Table 5), and layer scope below, with additional analyses deferred to Appendix F.

## 6 Scalability and Discussion

### 6.1 Scaling Properties across Model Capacities

We examine the scaling behavior of ROAST across models ranging from 0.6B to 32B parameters. Table 8 presents the results, showing that ROAST pro-

Model	Method	GSM8K	MATH500	IFEval
Qwen3-0.6B	Baseline	$48.86 \pm 0.19$	$33.59 \pm 0.47$	$62.46 \pm 1.27$
	Few-shot-20	$46.21 \pm 0.17$	$34.19 \pm 0.16$	-
	SADI	$56.30 \pm 0.85$	$36.25 \pm 2.34$	-
	CAA	$48.56 \pm 0.66$	$34.12 \pm 1.42$	-
Qwen3-8B	<b>ROAST</b>	$58.52 \pm 5.59$	$36.41 \pm 2.34$	$63.27 \pm 0.28$
	Baseline	$92.61 \pm 0.66$	$56.09 \pm 0.78$	$77.35 \pm 0.32$
	Few-shot-20	$92.46 \pm 0.75$	$57.38 \pm 0.35$	-
	SADI	$91.95 \pm 0.38$	$55.94 \pm 0.94$	-
ROAST	CAA	$90.06 \pm 0.09$	$52.56 \pm 1.22$	-
	<b>ROAST</b>	$92.95 \pm 0.14$	$57.79 \pm 1.14$	$80.50 \pm 1.98$

Table 2: Evaluation on reasoning and instruction-following benchmarks. Values denote accuracy (%)  $\pm$  standard deviation across 2 random seeds. **Bold**, underlined, and *italic* indicate the best, second-best, and third-best results, respectively. ROAST exhibits strong performance on multi-step reasoning tasks, particularly where base models show lower initial accuracy.

Component	GSM8K	MATH500	IFEval
MLP Activations	<b>59.86</b>	<b>37.34</b>	<b>63.27</b>
Attention Outputs	48.34	34.69	57.93
MLP + Attention	49.67	36.88	60.34

Table 3: Impact of steering different components (Qwen3-0.6B). MLP-based steering consistently outperforms attention-based steering.

Rollouts	SST2	MATH500
teacher-forced	$78.51 \pm 0.58$	$34.84 \pm 1.40$
8	$82.66 \pm 0.29$	$36.41 \pm 2.34$
64	<b><math>85.24 \pm 0.29</math></b>	$36.31 \pm 1.24$
128	$82.74 \pm 0.21$	<b><math>36.78 \pm 1.09</math></b>

Table 4: Impact of the number of rollouts on steering performance (Qwen3-0.6B).

vides consistent gains across scales. The efficacy extends beyond the Qwen family, with GLM4-32B showing a significant +12.11% absolute improvement on TruthfulQA, demonstrating its versatility across different architectures.

## 6.2 The Necessity of On-Distribution Intervention

Our results highlight the importance of distribution alignment between extraction and intervention. We hypothesize that teacher-forcing ( $p_{tf}$ ) introduces a “causal gap”: directions extracted from forced prefixes do not reliably align with the model’s natural auto-regressive manifold ( $p_{ar}$ ) at deployment. Empirically, methods that extract steering signals from on-distribution rollouts (ROC) yield consistent gains across tasks and model scales; in contrast, simply increasing diversity within teacher-forced data is insufficient to close this gap. This supports the interpretation that ROAST’s improve-

Anchor Position	SST2	MATH500
1	$78.75 \pm 0.27$	$34.46 \pm 1.25$
32	$83.14 \pm 2.81$	$34.11 \pm 0.18$
128	$84.62 \pm 0.99$	$33.04 \pm 0.54$
-1 (Last)	<b><math>85.24 \pm 0.29</math></b>	<b><math>36.41 \pm 2.34</math></b>

Table 5: Effect of steering vector anchor position. The final token position captures the most effective steering signal.

Layer Scope	SST2	MATH500
All Layers	<b><math>85.24 \pm 0.29</math></b>	<b><math>36.41 \pm 2.34</math></b>
First 5	$81.38 \pm 0.72$	$32.34 \pm 0.78$
Last 5	$81.02 \pm 0.36$	$33.13 \pm 1.87$

Table 6: Performance across different layer subsets. Intervening on all layers yields the best performance.

ments are driven by capturing the model’s *actual* reasoning trajectories—including its characteristic failure modes—which are largely absent under teacher-forcing. We further quantify this distributional shift by comparing mean activations under teacher-forcing versus rollouts. Figure 1 shows substantial discrepancies in mean activation directions (cosine similarity meaningfully below 1, with non-trivial relative  $L_2$  differences) across representative layers on both SST2 and GSM8K.

## 6.3 Comparison with Few-Shot Learning

ROAST achieves competitive performance with 100-shot in-context learning while requiring zero in-context examples at inference. This provides two advantages: (1) **Efficiency**: no prompt overhead, saving both context length and compute; (2) **Consistency**: steering is applied uniformly rather than depending on example selection and ordering effects that plague few-shot prompting.

Normalization	SST2	MATH500	TQA
None (only ROC)	$82.66 \pm 0.14$	$37.03 \pm 2.34$	$79.36 \pm 0.96$
Max	$82.66 \pm 0.29$	$36.41 \pm 2.34$	$79.97 \pm 0.87$
$L_2$	<b><math>85.24 \pm 0.29</math></b>	<b><math>37.34 \pm 1.72</math></b>	<b><math>81.18 \pm 0.17</math></b>

Table 7: Comparison of normalization strategies for CSS.

Model Size	IFEval	TruthfulQA
Qwen3-0.6B	$62.46 \pm 1.27$	$48.78 \pm 0.52$
ROAST-0.6B	<b><math>63.27 \pm 0.28</math></b>	<b><math>49.22 \pm 0.44</math></b>
Qwen3-8B	$78.47 \pm 1.70$	$78.66 \pm 0.78$
ROAST-8B	<b><math>80.50 \pm 1.98</math></b>	<b><math>81.18 \pm 0.17</math></b>
GLM4-9B	$81.02 \pm 0.12$	$53.83 \pm 0.01$
ROAST-9B	<b><math>81.82 \pm 0.42</math></b>	<b><math>60.10 \pm 0.17</math></b>
Qwen3-14B	$79.89 \pm 0.57$	$80.31 \pm 1.22$
ROAST-14B	<b><math>81.30 \pm 0.28</math></b>	<b><math>82.32 \pm 0.44</math></b>
Qwen3-32B	$80.31 \pm 0.14$	$85.39 \pm 0.21$
ROAST-32B	<b><math>81.02 \pm 0.71</math></b>	<b><math>86.64 \pm 0.21</math></b>
GLM4-32B	$80.31 \pm 0.71$	$57.40 \pm 1.66$
ROAST-32B	<b><math>81.11 \pm 0.71</math></b>	<b><math>69.51 \pm 3.83</math></b>

Table 8: Scaling behavior of ROAST across model capacities and architectures. Values denote accuracy (%)  $\pm$  standard deviation.

However, few-shot learning has complementary strengths: it can adapt instantly to new tasks without training, while ROAST requires one-time training. The optimal choice depends on deployment constraints—ROAST is preferable for high-throughput production settings, while few-shot suits rapid prototyping.

#### 6.4 Limitations of Linear Steering

ROAST, like other activation steering methods, assumes that task-relevant concepts can be captured via linear directions in activation space. This linear representation hypothesis (Park et al., 2024) is well-supported empirically but may not capture all forms of semantic content. Complex, non-linear transformations of information might require more sophisticated steering mechanisms. However, our consistent improvements across diverse tasks suggest that linear steering captures substantial signal for practical applications.

#### 6.5 Methodological Fairness and Comparison

We compare ROAST (on-distribution rollouts) with teacher-forcing baselines (CAA, SADI). This is the core methodological distinction: teacher forc-

ing induces a distribution shift that can degrade steering vectors, whereas rollouts estimate directions under the model’s own decoding distribution. For fairness, we match rollout/compute budgets when possible (e.g., ROAST-8 vs. CAA) and still observe consistent gains, indicating that improvements stem from higher-quality on-distribution signals rather than additional inference-time compute.

## 7 Conclusion

We presented ROAST, an activation-steering framework that mitigates distributional mismatch, improves task specificity, and reduces information loss. By introducing ROC and CSS, ROAST consistently improves performance across nine diverse benchmarks. Our findings underscore the importance of on-distribution analysis, showing that ROAST identifies semantically coherent directions grounded in the model’s natural manifold. Overall, ROAST provides a scalable and inference-efficient mechanism for modulating LLM behavior without fine-tuning or incurring context-window costs.

## Limitations

While ROAST establishes a robust framework for activation steering, we identify several limitations:

**Computational Complexity.** Let  $n$  be the number of training prompts,  $N$  the number of rollouts per prompt, and  $L$  the average rollout length (in tokens). ROAST requires  $O(nNL)$  decoding steps to generate rollouts, incurring higher cost than single-pass methods. For a 32B model, generating  $N=64$  rollouts for  $n=100$  prompts takes  $\sim 140$  seconds on a single H20 GPU with vLLM (Kwon et al., 2023) on MMLU, using a maximum generation length of 128 tokens. Nevertheless, our ablation study (Section 5.3) shows that ROAST remains competitive with as few as  $N=8$  rollouts, providing a practical trade-off between compute and estimation precision.

**Verifier Dependence.** ROC relies on task-specific verifiers  $\mathcal{V}(r, a^*)$ . This is straightforward for tasks that can be reliably *rewarded by a verifier* (i.e., where  $\mathcal{V}$  provides a meaningful scalar signal), but extending to open-ended generation (e.g., creative writing) requires more sophisticated validation, such as learned reward models (Stiennon et al., 2020) or reference-free metrics.

**Task Generalization.** Our experiments focus on classification and reasoning tasks with clear success criteria (Liang et al., 2023). While preliminary

results suggest potential in other areas, the efficacy of linear steering for highly creative or open-ended tasks remains an active area of investigation.

**Hyperparameter Sensitivity.** In our experiments, the intervention strength  $\alpha$  is selected via task-specific grid search, and performance can be sensitive to this choice across tasks. By contrast, we find the method is comparatively less sensitive to the specific intervention layer and component, and we rely on simple empirical heuristics (e.g., intervening on all MLP layers). More broadly, the *where* and *how* of applying a steering vector—e.g., which decoding step(s) to intervene on, and whether to add the vector only to the first generated token or to every generated token—remain underexplored design choices. Systematically optimizing the intervention position and schedule, together with other hyperparameters, is an important direction for future work.

## References

Yuntao Bai, Andy Jones, Kamal Ndousse, Amanda Askell, Anna Chen, Nova DasSarma, Dawn Drain, Stanislav Fort, Deep Ganguli, Tom Henighan, Nicholas Joseph, Saurav Kadavath, Jackson Kernion, Tom Conerly, Sheer El-Showk, Nelson Elhage, Zac Hatfield-Dodds, Danny Hernandez, Tristan Hume, and 12 others. 2022. [Training a helpful and harmless assistant with reinforcement learning from human feedback](#). *Preprint*, arXiv:2204.05862.

Zhongzhi Chen, Xingwu Sun, Xianfeng Jiao, Fengzong Lian, Zhanhui Kang, Di Wang, and Cheng-Zhong Xu. 2024. [Truth forest: Toward multi-scale truthfulness in large language models through intervention without tuning](#). *Preprint*, arXiv:2312.17484.

Karl Cobbe, Vineet Kosaraju, Mohammad Bavarian, Mark Chen, Heewoo Jun, Lukasz Kaiser, Matthias Plappert, Jerry Tworek, Jacob Hilton, Reiichiro Nakano, Christopher Hesse, and John Schulman. 2021. [Training verifiers to solve math word problems](#). *Preprint*, arXiv:2110.14168.

Alexis Conneau, Ruty Rinott, Guillaume Lample, Adina Williams, Samuel Bowman, Holger Schwenk, and Veselin Stoyanov. 2018. [XNLI: Evaluating cross-lingual sentence representations](#). In *Proceedings of the 2018 Conference on Empirical Methods in Natural Language Processing*, pages 2475–2485, Brussels, Belgium. Association for Computational Linguistics.

Team GLM, Aohan Zeng, Bin Xu, Bowen Wang, Chen-hui Zhang, Da Yin, Dan Zhang, Diego Rojas, Guanyu Feng, Hanlin Zhao, Hanyu Lai, Hao Yu, Hongning Wang, Jiadai Sun, Jiajie Zhang, Jiale Cheng, Jiayi Gui, Jie Tang, Jing Zhang, and 39 others. 2024. [Chatglm: A family of large language models from glm-130b to glm-4 all tools](#). *Preprint*, arXiv:2406.12793.

Dan Hendrycks, Collin Burns, Steven Basart, Andy Zou, Mantas Mazeika, Dawn Song, and Jacob Steinhardt. 2021a. [Measuring massive multitask language understanding](#). *Preprint*, arXiv:2009.03300.

Dan Hendrycks, Collin Burns, Saurav Kadavath, Akul Arora, Steven Basart, Eric Tang, Dawn Song, and Jacob Steinhardt. 2021b. [Measuring mathematical problem solving with the math dataset](#). *Preprint*, arXiv:2103.03874.

Peter J Huber and Elvezio M Ronchetti. 2009. *Robust Statistics*. Wiley.

Woosuk Kwon, Zhuohan Li, Siyuan Zhuang, Ying Sheng, Lianmin Zheng, Cody Hao Yu, Joseph E. Gonzalez, Hao Zhang, and Ion Stoica. 2023. Efficient memory management for large language model serving with pagedattention. In *Proceedings of the ACM SIGOPS 29th Symposium on Operating Systems Principles*.

Kenneth Li, Oam Patel, Fernanda Viégas, Hanspeter Pfister, and Martin Wattenberg. 2024. [Inference-time intervention: Eliciting truthful answers from a language model](#). *Preprint*, arXiv:2306.03341.

Percy Liang, Rishi Bommasani, Tony Lee, Dimitris Tsipras, Dilara Soylu, Michihiro Yasunaga, Yian Zhang, Deepak Narayanan, Yuhuai Wu, Ananya Kumar, Benjamin Newman, Binhang Yuan, Bobby Yan, Ce Zhang, Christian Cosgrove, Christopher D. Manning, Christopher Ré, Diana Acosta-Navas, Drew A. Hudson, and 31 others. 2023. [Holistic evaluation of language models](#). *Preprint*, arXiv:2211.09110.

Stephanie Lin, Jacob Hilton, and Owain Evans. 2022. [TruthfulQA: Measuring how models mimic human falsehoods](#). In *Proceedings of the 60th Annual Meeting of the Association for Computational Linguistics (Volume 1: Long Papers)*, pages 3214–3252, Dublin, Ireland. Association for Computational Linguistics.

Sheng Liu, Haotian Ye, Lei Xing, and James Zou. 2024. [In-context vectors: Making in context learning more effective and controllable through latent space steering](#). *Preprint*, arXiv:2311.06668.

Kiho Park, Yo Joong Choe, and Victor Veitch. 2024. [The linear representation hypothesis and the geometry of large language models](#). In *Proceedings of the 41st International Conference on Machine Learning*, volume 235 of *Proceedings of Machine Learning Research*, pages 39643–39666. PMLR.

Nina Rimsky, Nick Gabrieli, Julian Schulz, Meg Tong, Evan Hubinger, and Alexander Turner. 2024. [Steering llama 2 via contrastive activation addition](#). In *Proceedings of the 62nd Annual Meeting of the Association for Computational Linguistics (Volume 1: Long Papers)*, pages 15504–15522, Bangkok, Thailand. Association for Computational Linguistics.

Keisuke Sakaguchi, Ronan Le Bras, Chandra Bhagavatula, and Yejin Choi. 2021. [Winogrande: an adversarial winograd schema challenge at scale](#). *Commun. ACM*, 64(9):99–106.

Richard Socher, Alex Perelygin, Jean Wu, Jason Chuang, Christopher D. Manning, Andrew Ng, and Christopher Potts. 2013. [Recursive deep models for semantic compositionality over a sentiment treebank](#). In *Proceedings of the 2013 Conference on Empirical Methods in Natural Language Processing*, pages 1631–1642, Seattle, Washington, USA. Association for Computational Linguistics.

Nisan Stiennon, Long Ouyang, Jeff Wu, Daniel M. Ziegler, Ryan Lowe, Chelsea Voss, Alec Radford, Dario Amodei, and Paul Christiano. 2020. Learning to summarize from human feedback. In *Proceedings of the 34th International Conference on Neural Information Processing Systems*, NIPS ’20, Red Hook, NY, USA. Curran Associates Inc.

Alessandro Stolfo, Vidhisha Balachandran, Safoora Yousefi, Eric Horvitz, and Besmira Nushi. 2025. [Improving instruction-following in language models through activation steering](#). *Preprint*, arXiv:2410.12877.

Nishant Subramani, Nivedita Suresh, and Matthew Peters. 2022. [Extracting latent steering vectors from pretrained language models](#). In *Findings of the Association for Computational Linguistics: ACL 2022*, pages 566–581, Dublin, Ireland. Association for Computational Linguistics.

Mingjie Sun, Xinlei Chen, J. Zico Kolter, and Zhuang Liu. 2024. [Massive activations in large language models](#). *Preprint*, arXiv:2402.17762.

Gemma Team, Aishwarya Kamath, Johan Ferret, Shreya Pathak, Nino Vieillard, Ramona Merhej, Sarah Perrin, Tatiana Matejovicova, Alexandre Ramé, Morgane Rivière, Louis Rouillard, Thomas Mesnard, Geoffrey Cideron, Jean bastien Grill, Sabela Ramos, Edouard Yvinec, Michelle Casbon, Etienne Pot, Ivo Penchev, and 197 others. 2025. [Gemma 3 technical report](#). *Preprint*, arXiv:2503.19786.

Alexander Matt Turner, Lisa Thiergart, Gavin Leech, David Udell, Juan J. Vazquez, Ulisse Mini, and Monte MacDiarmid. 2024. [Steering language models with activation engineering](#). *Preprint*, arXiv:2308.10248.

Weixuan Wang, Jingyuan Yang, and Wei Peng. 2025. [Semantics-adaptive activation intervention for llms via dynamic steering vectors](#). *Preprint*, arXiv:2410.12299.

Jason Wei, Maarten Bosma, Vincent Y. Zhao, Kelvin Guu, Adams Wei Yu, Brian Lester, Nan Du, Andrew M. Dai, and Quoc V. Le. 2022. [Finetuned language models are zero-shot learners](#). *Preprint*, arXiv:2109.01652.

An Yang, Anfeng Li, Baosong Yang, Beichen Zhang, Binyuan Hui, Bo Zheng, Bowen Yu, Chang Gao, Chengen Huang, Chenxu Lv, Chujie Zheng, Dayiheng Liu, Fan Zhou, Fei Huang, Feng Hu, Hao Ge, Haoran Wei, Huan Lin, Jialong Tang, and 41 others. 2025. [Qwen3 technical report](#). *Preprint*, arXiv:2505.09388.

Jeffrey Zhou, Tianjian Lu, Swaroop Mishra, Siddhartha Brahma, Sujoy Basu, Yi Luan, Denny Zhou, and Le Hou. 2023. [Instruction-following evaluation for large language models](#). *Preprint*, arXiv:2311.07911.

Andy Zou, Long Phan, Sarah Chen, James Campbell, Phillip Guo, Richard Ren, Alexander Pan, Xuwang Yin, Mantas Mazeika, Ann-Kathrin Dombrowski, Shashwat Goel, Nathaniel Li, Michael J. Byun, Zifan Wang, Alex Mallen, Steven Basart, Sanmi Koyejo, Dawn Song, Matt Fredrikson, and 2 others. 2025. [Representation engineering: A top-down approach to ai transparency](#). *Preprint*, arXiv:2310.01405.

## A Implementation Details

### A.1 Rollout-based On-distribution Contrastive Pair Generation (ROC)

Algorithm 1 details the process of generating on-distribution contrastive pairs using model rollouts.

---

#### Algorithm 1 Rollout-based On-distribution Contrastive Pair Generation (ROC)

---

**Require:** Training samples  $\{(q_i, a_i^+)\}_{i=1}^N$ , number of rollouts  $n$ , temperature  $T$   
**Ensure:** Contrastive pairs  $\mathcal{P} = \{(r^+, r^-)\}$

- 1:  $\mathcal{P} \leftarrow \emptyset$
- 2: **for** each sample  $(q_i, a_i^+)$  **do**
- 3:   Generate  $n$  responses:  $\{r_1, \dots, r_n\} \sim p_{\text{par}}(\cdot | q_i)$  with temperature  $T$
- 4:   Classify:  $\mathcal{R}^+ \leftarrow \{r_j : \text{correct}(r_j, a_i^+)\}$ ,  $\mathcal{R}^- \leftarrow \{r_j : \neg \text{correct}(r_j, a_i^+)\}$
- 5:   **if**  $\mathcal{R}^+ = \emptyset$  **then**
- 6:     Use re-read:  $\mathcal{R}^+ \leftarrow \{a_i^+\}$ , mark as re-read with weight  $w_{\text{fallback}}$
- 7:   **end if**
- 8:   **if**  $\mathcal{R}^- = \emptyset$  **then**
- 9:     Skip sample (model always correct)
- 10:   **end if**
- 11:   Form pairs:  $\mathcal{P}_i \leftarrow \{(r^+, r^-) : r^+ \in \mathcal{R}^+, r^- \in \mathcal{R}^-\}$
- 12:    $\mathcal{P} \leftarrow \mathcal{P} \cup \mathcal{P}_i$
- 13: **end for**
- 14: **return**  $\mathcal{P}$

---

### A.2 Dataset Preparation and Loading

We utilize a unified dataset loader to process diverse benchmarks, categorizing them into two

modes to match our rollout configuration: For all tasks, we construct a **Steering Set** by randomly sampling  $N = 100$  examples (or  $N = 1000$ ) from the training data. The ground truth is used solely for verifying the correctness of rollouts (via verifier) rather than for creating teacher-forced pairs.

### A.3 Rollout and Steering Configuration

The primary experimental settings for ROAST across all models are:

- **Rollout Generation:** We use task-specific rollout counts ( $n = 64$  for base-mode tasks,  $n = 8$  for chat-mode tasks) per training sample, utilizing nucleus sampling ( $p = 0.9$ ) and temperature  $T = 0.8$ .
- **Steering Components:** Interventions are applied to MLP activations across all layers by default. We also evaluated attention outputs (see Figure 7).
- **Continuous Soft Scaling (CSS):**  $L_2$  normalization is the default strategy for computing scaling weights  $\beta$ .

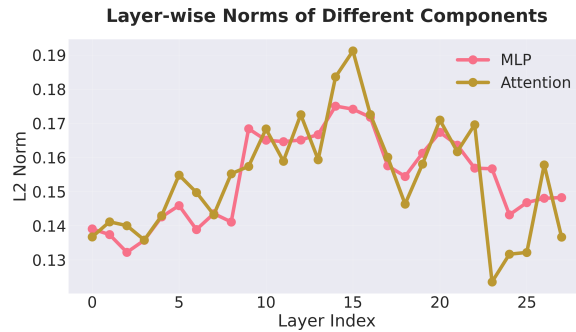


Figure 7: Performance comparison of steering different model components (MLP vs Attention). MLP steering yields the most robust improvements.

- **Aggregation:** Grouped normalization (one question, one vote) is used to ensure balanced contribution from all training samples.
- **Training Data:** 100 or 1000 samples per dataset are used to estimate steering vectors.

### A.4 Evaluation Protocol

All evaluations use greedy decoding to ensure reproducibility, and we adopt the standard evaluation protocols from the respective original papers to ensure comparability. For multiple-choice tasks like MMLU (Hendrycks et al., 2021a), we compare the model’s log-probabilities for the choice

tokens (A, B, C, D). For generation-centric tasks, including TruthfulQA (MC1) (Lin et al., 2022) and IFEval (Zhou et al., 2023), we use generation-based evaluation: for MC1, we extract the choice letter from the model’s generated response (optionally using \boxed markers); for IFEval, we apply a suite of 25+ automated verification functions to the generated text to check for instruction compliance. Mathematical reasoning (GSM8K, MATH500) (Cobbe et al., 2021; Hendrycks et al., 2021b) utilizes symbolic equivalence checking to verify the final answer.

### A.5 Datasets and Metrics

We evaluate ROAST on 9 datasets covering diverse capabilities. For all datasets, we employ a rigorous train/dev/test split strategy to ensure fair evaluation and avoid test data leakage. Specifically, we randomly sample  $N = 100$  (or  $N = 1000$  for specific ablation studies) examples from the training set (or validation set if training is unavailable) to serve as the **Steering Set** for vector extraction. The remaining data is split into a **Dev Set** (typically 20%) for hyperparameter tuning and a **Test Set** (typically 80%) for final evaluation. Table 9 provides the exact sample counts for each dataset.

Dataset	Total Eval Samples	Steering Set	Split (Dev / Test)	Source
SST2	872	100/1000	174 / 698	GLUE Dev
SST5	2,210	100/1000	442 / 1,768	Test
MMLU	11,173	100/1000	2,234 / 8,939	Test
TruthfulQA	717	100/1000	143 / 574	Validation
Winogrande	1,267	100/1000	253 / 1,014	Dev
XNLI	5,010	100/1000	1,002 / 4,008	Test
GSM8K	1,319	100	263 / 1,056	Test
MATH500	400	100	80 / 320	Test
IFEval	441	100	88 / 353	-

Table 9: Detailed statistics of dataset splits. **Total Eval Samples** refers to the number of samples available for evaluation (excluding the Steering Set). **Steering Set** sizes of 1000 are used in specific ablation studies (e.g., grouped normalization analysis). **Split** indicates the number of samples used for hyperparameter tuning (Dev) versus final reporting (Test).

- **Truthfulness (MC1):** For TruthfulQA, we use the *MC1 (Single-True)* evaluation protocol. The model is presented with a question and four options, where only one is correct. A response is considered correct if the model identifies the unique truthful answer.
- **Instruction Following (Prompt-level strict):** For IFEval, we report *Prompt-level strict accuracy*. This requires the model to satisfy *all* verifiable constraints (e.g., word count, formatting, keyword inclusion) within a prompt.

- **Sentiment Analysis:** SST2, SST5.
- **Reasoning:** MMLU (Multi-task), GSM8K, MATH500 (Mathematical).
- **Commonsense & NLI:** Winogrande, XNLI.

## A.6 Baseline Hyperparameter Tuning

To ensure fair comparison, both CAA and SADI are tuned over steering strengths  $\{1e-3, 2e-2, 3, 5, 10\}$ . SADI additionally undergoes a search over top- $k$  values  $\{5, 10, 50, 100\}$  following its original paper’s recommendations.

## B Why Normalize Twice? A Note on Grouped Mean Normalization

Grouped Mean Normalization implements a simple principle—*one question, one vote*—by separating the estimation of a steering *direction* from the choice of an intervention *magnitude*. Concretely, it applies normalization at two different aggregation levels, each addressing a distinct failure mode.

**Per-question normalization: preventing “loud” prompts from dominating.** For each question  $q$ , we first average the difference vectors over its rollout-pair set  $\mathcal{P}_q$  and then normalize:

$$\bar{v}_q = \text{Norm} \left( \frac{1}{|\mathcal{P}_q|} \sum_{(r^+, r^-) \in \mathcal{P}_q} (h(r^+) - h(r^-)) \right).$$

This step is motivated by the empirical observation that activation magnitudes can vary dramatically across prompts in LLMs: some prompts induce large internal changes while others yield much smaller responses. Without per-question normalization, a global mean over all rollout pairs can be dominated by a small subset of “high-amplitude” questions (or questions that admit many rollout pairs), causing the resulting steering vector to reflect amplitude outliers rather than the semantic *consensus direction*. Per-question normalization therefore enforces that each question contributes primarily its *direction* (i.e., its local contrastive signal) rather than its raw scale.

**Global normalization: decoupling direction agreement from intervention strength.** We then average the unit directions across questions,

$$v_{\text{avg}} = \frac{1}{|Q|} \sum_{q \in Q} \bar{v}_q,$$

and optionally apply a final normalization  $v_{\text{final}} = \text{Norm}(v_{\text{avg}})$ . Note that  $\|v_{\text{avg}}\| \leq 1$  by construction: it approaches 1 when per-question directions are highly aligned and shrinks toward 0 when they disagree. If we were to use  $v_{\text{avg}}$  directly for intervention, the *effective* steering magnitude would implicitly depend on this directional agreement, making the strength hyperparameter (e.g., a coefficient  $\alpha$  in the intervention) difficult to interpret and tune across datasets and settings. The final normalization standardizes the steering vector to a unit direction, ensuring that the intervention magnitude is controlled explicitly by the user-specified strength rather than by incidental variation in directional coherence.

**Takeaway.** The first normalization improves robustness of *estimation* (equalizing question contributions), while the second normalization improves usability of *deployment* (standardizing the vector passed to the model). Together, they yield a stable direction estimate and a clean separation between “where to steer” and “how strongly to steer.”

## C Contrastive Showcases

We present specific examples where ROAST successfully steers the model to correct reasoning or classification when the baseline model fails. These showcases highlight ROAST’s ability to correct semantic misunderstandings and logical errors in both chat and generation modes.

### C.1 Chat Mode: Mathematical Reasoning (GSM8K)

**Question:** Thomas has \$1000 in \$20 bills. He loses 10 bills. He uses half of the remaining bills to pay for a bill. He then triples his money. He converts all his bills to \$5 bills. How many \$5 bills does he have?

**Baseline Response (Incorrect):**

1. Thomas starts with \$1000 in 20 dollar bills.
2. He loses 10 bills, so he has  $\$1000 - 10 = 990$  dollars left. (Error: Subtracts number of bills from total value)
3. He uses half of the remaining bills to pay for a bill:  $990/2 = 495$  dollars. ... **Final Answer:** 74

**ROAST Response (Correct):**

To solve the problem, we need to track Thomas’s money and bills step by step.

- Initial Setup:** Thomas has \$1000 in 20-dollar bills. - He loses 10 bills, so he has  $\$1000 - 10 \times 20 = \$800$  remaining. **(Correct: Converts bills to value before subtraction)**
- After Losing Bills:** - He uses half of the remaining bills...  $800/2 = 400$ .
- Tripling His Money:**  $400 \times 3 = 1200$ .
- Converting to 5-Dollar Bills:**  $1200/5 = 240$ . **Final Answer:** 240

## C.2 Generation Mode: Sentiment Analysis (SST2)

**Input:** the piquant story needs more dramatic meat on its bones

### Baseline Response (Incorrect):

positive

The sentence expresses a positive sentiment, indicating that the story needs more substance, which implies a desire for improvement but frames it constructively.

### ROAST Response (Correct):

negative

The sentence "the piquant story needs more dramatic meat on its bones" expresses a negative sentiment because it criticizes the story for lacking sufficient depth or substance ("dramatic meat").

## D Reasoning Showcase

In this section, we provide detailed examples of ROAST's performance on complex reasoning tasks from the MATH500 dataset using Qwen3-0.6B. These examples demonstrate the model's ability to maintain logical coherence and arrive at correct solutions under activation steering.

### D.1 Example 1: Inverse Proportionality

**Question:** The popularity of a television (measured in number of sales) is inversely proportional to its cost. If a television costing \$1500 has a popularity of 15 customers, what is the popularity of a television costing \$2500?

### Model Response (Steered):

*Step 1: Use the relationship between popularity and cost.* Let  $P$  = popularity and  $C$  = cost. Since popularity is inversely proportional to cost,  $P \cdot C = k$ . *Step 2:*

*Find the constant  $k$ .*  $15 \cdot 1500 = 22500$ .  
*Step 3: Solve for the new popularity*  $P'$ .  $P' \cdot 2500 = 22500 \Rightarrow P' = 22500/2500 = 9$ . **Final Answer:** 9

## D.2 Example 2: Arithmetic with Fractions

**Question:** Simplify  $\frac{1}{5} \cdot \frac{8}{7} \div \frac{12}{20}$ .

### Model Response (Steered):

- Multiply the first two fractions:  $\frac{1}{5} \cdot \frac{8}{7} = \frac{8}{35}$ .
- Divide by the third fraction (multiply by its reciprocal):  $\frac{8}{35} \div \frac{12}{20} = \frac{8}{35} \cdot \frac{20}{12}$ .
- Multiply numerators and denominators:  $\frac{8 \cdot 20}{35 \cdot 12} = \frac{160}{420}$ .
- Simplify:  $\frac{160}{420} = \frac{16}{42} = \frac{8}{21}$ . **Final Answer:**  $\frac{8}{21}$

## D.3 Example 3: Coordinate Geometry (Reflections)

**Question:** Reflect the point  $(0, 0)$  over the vertical line  $x = 1$ , then reflect the resulting point over the horizontal line  $y = 2$ . What are the final coordinates?

### Model Response (Steered):

*Step 1: Reflect  $(0, 0)$  over  $x = 1$ .* The reflection over  $x = a$  is  $(2a - x, y)$ . Here  $a = 1$ , so  $(0, 0) \rightarrow (2(1) - 0, 0) = (2, 0)$ . *Step 2: Reflect  $(2, 0)$  over  $y = 2$ .* The reflection over  $y = b$  is  $(x, 2b - y)$ . Here  $b = 2$ , so  $(2, 0) \rightarrow (2, 2(2) - 0) = (2, 4)$ . **Final Answer:**  $(2, 4)$

## D.4 Example 4: Algebraic Factoring

**Question:** Factor the expression  $ab + 5b + 2a + 10$ .

### Model Response (Steered):

- Step 1: Group terms.*  $ab + 2a + 5b + 10$ .
- Step 2: Factor out  $a$  from the first two terms and 5 from the last two.*  $a(b + 2) + 5(b + 2)$ .
- Step 3: Factor out the common term  $(b + 2)$ .*  $(a + 5)(b + 2)$ . **Final Answer:**  $(a + 5)(b + 2)$

## E Methodological Details

### E.1 Normalization Strategies for CSS

We investigate two primary strategies for continuous soft scaling:

- $L_2$  Normalization:** defined as  $\text{Norm}(\Delta h) = \Delta h / \|\Delta h\|_2$ . This projects the difference vector onto the unit hypersphere, ensuring the total energy is normalized to unity while preserving the exact directional information.

- **Max Normalization:** defined as  $\text{Norm}(\Delta h) = \Delta h / \|\Delta h\|_\infty$ . This scales the vector such that the maximum absolute component is 1, preventing individual dimensions from producing out-of-distribution activation magnitudes.

## E.2 Grouped Mean Normalization Aggregation

The process consists of two stages of normalization to maintain both directional consensus and numerical stability:

### 1. Intra-question Group Mean Aggregation:

For each question  $q$ , we compute the mean of its contrastive pairs and apply normalization:

$$\bar{v}_q = \text{Norm} \left( \frac{1}{|\mathcal{P}_q|} \sum_{(r^+, r^-) \in \mathcal{P}_q} (h(r^+) - h(r^-)) \right)$$

- 2. **Global Consensus Aggregation:** We average these normalized group means and apply a final normalization to obtain the task-level steering vector:  $v_{\text{final}} = \text{Norm} \left( \frac{1}{|Q|} \sum_{q \in Q} \bar{v}_q \right)$ .

## F Additional Analysis

### F.1 Representational Dynamics and Layer Specificity

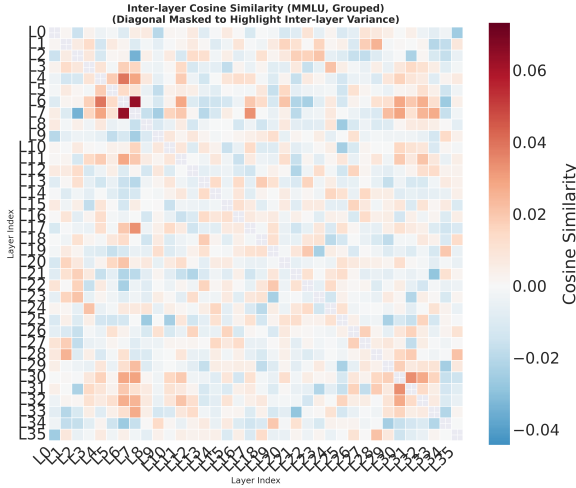


Figure 8: Inter-layer Cosine Similarity of steering vectors (MMLU). The heatmap reveals near-zero similarity (scale  $\pm 0.06$ ) between distinct layers, indicating that ROAST extracts highly layer-specific semantic directions orthogonal to each other, necessitating precise layer-wise intervention.

We investigate the evolution of steering directions across the model’s depth. Figure 8 presents

the inter-layer cosine similarity matrix. Contrary to the hypothesis of a continuous global "truth direction," we observe that steering vectors from different layers are effectively orthogonal (similarity  $\approx 0$ ). This suggests that the model’s representation undergoes significant transformation layer-by-layer, and ROAST successfully captures these distinct, layer-specific semantic axes rather than a generic global feature.

## F.2 Task Specificity and Orthogonality

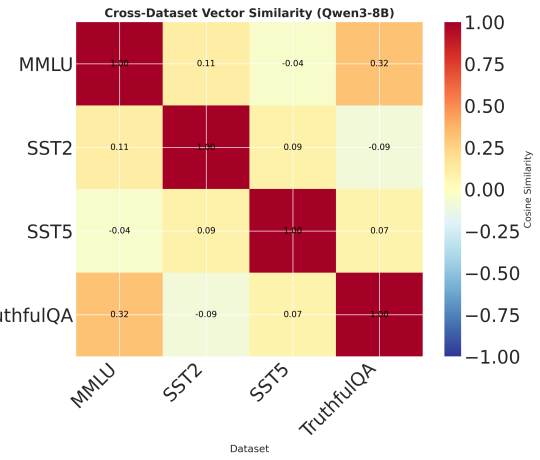


Figure 9: Cross-dataset cosine similarity (Qwen3-8B). Even between related tasks (e.g., SST2 vs SST5), the steering vectors exhibit low similarity ( $< 0.1$ ), demonstrating that ROAST learns fine-grained, distribution-specific features rather than broad task-category concepts.

To assess the granularity of the learned representations, we compute the cross-dataset similarity of steering vectors (Figure 9). Surprisingly, we find that the learned vectors are highly task-specific. Even between conceptually similar tasks like SST2 and SST5 (both sentiment analysis), the cosine similarity is low ( $\sim 0.09$ ). This orthogonality implies that ROAST is not overfitting to a superficial "sentiment" or "reasoning" template, but is instead extracting precise, distribution-dependent features unique to each dataset’s underlying logic.

## F.3 Extended Ablation Studies

We provide additional ablation studies on grouped normalization across different model sizes.

## F.4 Additional Visualization

Model	Train Size	Grouped Avg	No-group Avg
Qwen3-0.6B	100	<b>50.03</b>	49.22
Qwen3-0.6B	1000	<b>49.11</b>	48.52
Qwen3-8B	100	68.78	<b>69.48</b>
Qwen3-8B	1000	<b>70.22</b>	69.33
Gemma3-1B	100	<b>47.26</b>	46.86
Gemma3-1B	1000	47.82	<b>48.09</b>

Table 10: Grouped versus non-grouped normalization across model sizes (average accuracy over SST2, SST5, MMLU, TruthfulQA, Winogrande, XNLI).

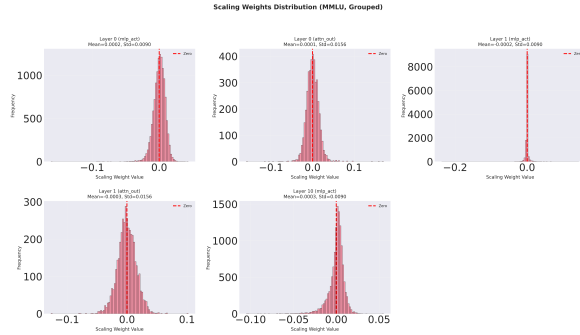


Figure 10: Layer-wise scaling weights under **grouped** normalization in Qwen3-8B.

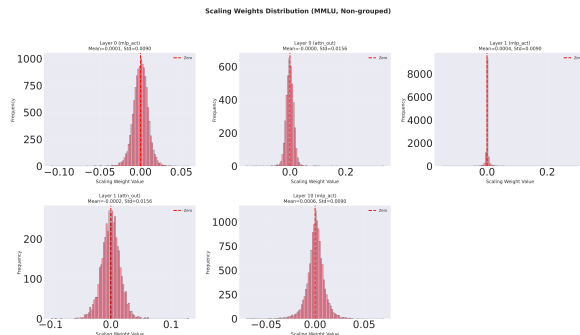


Figure 11: Layer-wise scaling weights under **non-grouped** normalization in Qwen3-8B.

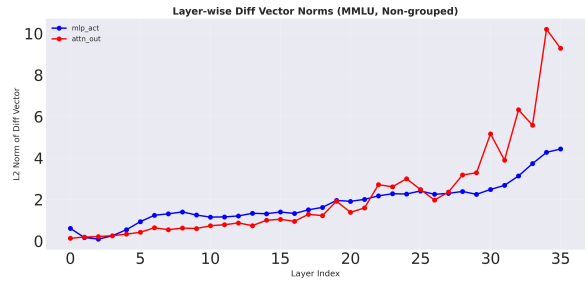


Figure 13: Layer-wise diff vector norms under **non-grouped** normalization in Qwen3-8B.

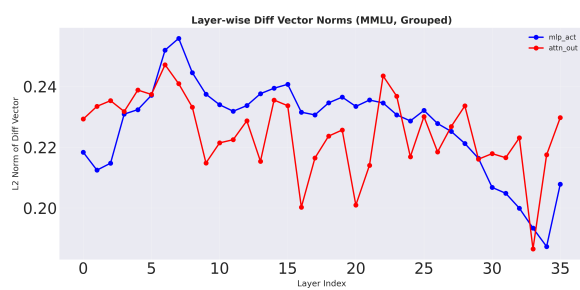


Figure 12: Layer-wise diff vector norms under **grouped** normalization in Qwen3-8B.